Chemical Science

ROYAL SOCIETY OF CHEMISTRY

EDGE ARTICLE

View Article Online
View Journal

Cite this: DOI: 10.1039/d6sc02674e

All publication charges for this article have been paid for by the Royal Society of Chemistry

Received 1st April 2026
Accepted 22nd May 2026

DOI: 10.1039/d6sc02674e

rsc.li/chemical-science

Boron buckminsterfullerene

Hyun Wook Choi,†[a] Yang-Yang Zhang,†[b] Deniz Kahraman,[a] Cong-Qiao Xu,[c] Han-Wen Gao,[a] Jun Li *[bcd] and Lai-Sheng Wang *[a]

Fullerenes, spherical molecules made entirely of carbon atoms, have played a foundational role in the birth of nanoscience. Despite extensive research, however, comparable structures composed of other elements have remained elusive, highlighting the unique bonding properties of carbon that enable the formation of such remarkable nanoscale architectures. Here we report the observation of an 80-atom boron fullerene using photoelectron spectroscopy. The photoelectron spectrum of B_{80}^- reveals a surprisingly simple spectral pattern, suggesting a high symmetry B_{80} cluster with a sizable energy gap. Among the low-lying structures, only the simulated spectrum of the B_{80}^- buckyball is found to agree with the experimental result. We show that the electronic structure and chemical bonding of the B_{80} buckyball closely mimic those of the C_{60} buckminsterfullerene. The discovery of the B_{80} boron buckminsterfullerene will stimulate its bulk synthesis and pave the way for the development of potential boron-fullerene chemistry and materials.

1 Introduction

Carbon is known to form a range of amazing nanostructures from the C_{60} buckminsterfullerene to carbon nanotubes and graphene.[1–3] There has been immense interest in the search for analogous nanostructures composed of other elements. Owing to the strong boron–boron bonding, boron is a particularly promising candidate. Inspired by this prospect, we have been investigating the structures and bonding of size-selected boron clusters over the past two decades using anion photoelectron spectroscopy (PES) in combination with quantum chemical calculations.[4–8] Boron cluster anions (B_x^-) have been found to be planar for at least up to B_{42}^-,[9] in sharp contrast to bulk boron allotropes, which consist of different polyhedral building blocks, in particular the B_{12} icosahedron, as a consequence of boron's electron deficiency.[10–12] For cationic boron clusters (B_x^+), tubular structures are possible above B_{16}^+.[13,14] The discovery of the planar B_{36} cluster with a central hexagonal vacancy provided the first experimental evidence for the viability of borophene,[15] which has since been synthesized on inert substrates.[16,17] The B_{40} cluster was first found to adopt a fullerene-like cage structure with D_{2d} symmetry, composed of triangles, hexagons, and heptagons,[18] even though the global minimum of B_{40}^- remains planar. Beyond B_{40}^-, the B_{41}^- and B_{42}^- clusters were found to be planar,[9] whereas the B_{48}^- cluster adopts a double layer structure.[19,20] A recent joint PES, chemisorption, and theoretical study showed that the 2D–3D transition occurs at B_{46}^- and that the iconic bulk-like B_{12} unit appears in the B_{56}^- cluster.[21]

Although the B_{60} cluster cannot adopt the soccer-ball structure of C_{60} because of boron's electron deficiency,[22] a fullerene-like B_{80} cluster was intriguingly proposed by placing one B atom in each of the 20 hexagons of a soccer-ball-shaped B_{60} framework.[23] Subsequent density functional theory (DFT) calculations, however, indicated that the B_{80} buckyball is significantly less stable than core–shell or other low-symmetry cage structures.[24–31] Thus, despite the discovery of the smaller B_{40} fullerene,[18] the existence of a B_{80} buckyball has remained questionable. Experimentally, we have found that, with increasing cluster size, photoelectron spectra of size-selected B_x^- clusters become exceedingly complicated or featureless due to challenges in cluster cooling and possible co-existence of low-lying isomers.[21] These complications made it difficult to use photoelectron spectra as electronic fingerprints for elucidating the structures and bonding of larger boron clusters.

Here we report the surprising observation that the photoelectron spectrum of the B_{80}^- cluster exhibits simple, well-resolved features, suggesting a highly symmetric and stable B_{80} cluster with a large energy gap. We carried out extensive global minimum structural searches at the DFT level. Among the low-lying candidate structures, only the simulated spectrum of the B_{80}^- buckyball agrees with the experimental results. The corresponding neutral B_{80} has the I_h symmetry, as proposed previously.[23] Chemical bonding analyses reveal both three-center and four-center delocalized bonds for the B_{80} buckyball, which are shown to completely mimic the localized bonding in C_{60}.

[a]Department of Chemistry, Brown University, Providence, Rhode Island 02912, USA. E-mail: lai-sheng_wang@brown.edu

[b]Fundamental Science Center of Rare Earths, Ganjiang Innovation Academy, Chinese Academy of Sciences, Ganzhou 341000, China. E-mail: junli@tsinghua.edu.cn

[c]Department of Chemistry and Provincial Key Laboratory of Catalytic Chemistry, Southern University of Science and Technology, Shenzhen 518055, China

[d]Department of Chemistry and Engineering Research Center of Advanced Rare-Earth Materials of Ministry of Education, Tsinghua University, Beijing 100084, China

† These authors contributed equally to this work.

2 Results

2.1 Photoelectron spectroscopy

We produced boron clusters using a laser vaporization supersonic cluster source with helium as the carrier gas (see the SI for details). To achieve more effective cooling of large clusters, we tested helium seeded with different amounts of argon,[21] which enhances collisional cooling efficiency. Using helium seeded with 20% argon, we obtained a completely unexpected simple photoelectron spectrum for B_{80}^- (Fig. 1a). The spectrum displays three well-resolved bands, X, A, and B; a slightly better resolved spectrum for the X and A bands was also obtained at a lower photon energy (Fig. S1). The weak X band corresponds to electron detachment from the ground state of B_{80}^- to the ground state of neutral B_{80}: the onset of band X gives an adiabatic detachment energy (ADE) of 3.1 eV, which is also the electron affinity (EA) of neutral B_{80}. The first vertical detachment energy (VDE_1), measured from the maximum of band X, is 3.2 eV, while the VDEs of bands A and B are 4.0 eV and 4.8 eV, respectively. Beyond band B, the spectrum becomes increasingly congested, indicating a high density of electronic states.

We note that this well-resolved photoelectron spectrum of B_{80}^- exhibits some similarity to that of the C_{60}^- buckminsterfullerene produced from a laser vaporization cluster source.[32] The X–A separation of 0.8 eV defines the energy gap between the highest occupied (HOMO) and the lowest unoccupied (LUMO) molecular orbitals of B_{80}. The relatively large HOMO–LUMO gap of B_{80} implies that it is a highly stable electronic system. We have found that the photoelectron spectra of B_x^- clusters with $x > 50$ are extremely complicated and congested, as shown recently in the case of B_{56}^-.[21] The uniqueness of the B_{80}^- spectrum is unprecedented and unexpected for such a large boron cluster, which is reminiscent of the unique photoelectron spectrum of C_{60}^- among the large C_x^- clusters.[32] The simple and well-resolved photoelectron spectral features suggest: (1) high degeneracies in the electronic energy levels of B_{80}^- as a result of high symmetry and (2) there are no significant contributions from other low-lying isomers which would have smeared out the spectral features.

2.2 Global minimum structural searches at DFT level

A number of computational studies have been carried out previously on B_{80} at the DFT level.[25–31] In addition to the originally proposed B_{80} buckyball,[23] cage structures involving filling the pentagons and core-shell-type structures were shown to be more stable. To understand the observed photoelectron spectrum and to see if there are other high symmetry low-lying isomers, we have performed additional global minimum searches for the B_{80}^- anion and neutral B_{80} using the constrained basin-hopping algorithm in the TGMin (v3.0) program[33] and optimized the low-lying isomers at the B3LYP/6-31G(d) level (see the SI for details). The structures within 13 eV of the global minimum at the B3LYP level for B_{80}^- and B_{80} are given in Figs. S2 and S3, respectively.

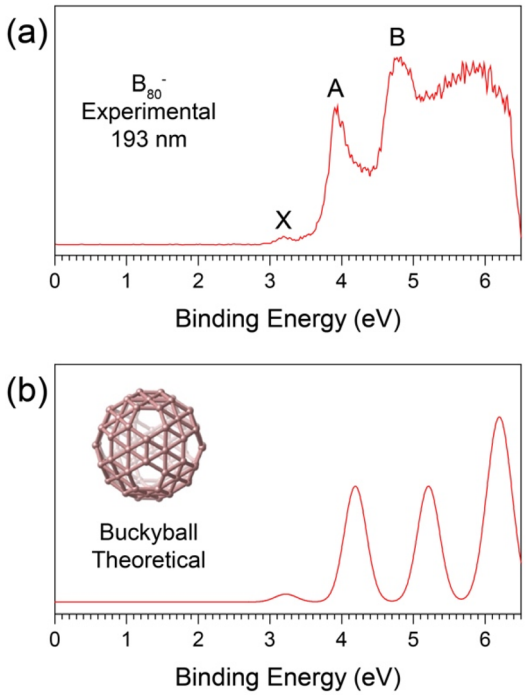

Fig. 1 (a) The experimental photoelectron spectrum of B_{80}^- at 193 nm (6.424 eV). (b) The simulated spectrum of the B_{80}^- buckyball by using the generalized Koopmans' theorem.

We find many new low-lying structures that have not been reported before. In particular, we find that a planar structure with four hexagonal vacancies is the global minimum for both B_{80}^- and B_{80} at the B3LYP level. The low-lying isomers are populated with many planar structures with different arrangements of the hexagons, highlighting the stability of borophenes.[15,34] A core–shell structure is found to be close in energy with the planar global minimum for B_{80}^- (Fig. S2). The neutral B_{80} has similar low-lying isomers as the anion (Fig. S3), but the core–shell structure is only 0.02 eV higher in energy. A D_{3d} cage for B_{80}^- is found to be 1.06 eV above the planar global minimum, whereas the B_{80}^- buckyball (D_{5d}) is 3.41 eV higher at the B3LYP level of theory. Eight other cage structures, as well as seven other planar structures, two other core–shell structures and a double-ring structure, are found to be more stable than the D_{5d} B_{80}^- buckyball (Fig. S2). For neutral B_{80}, aside from the planar and double-ring structures, our computational results for the core–shell and cage structures at the B3LYP level are consistent with previous DFT studies.[25–31]

We did further DFT calculations for selected low-lying isomers of neutral B_{80} using different functionals, including the planar structure, the core–shell structure, the buckyball, the double ring, as well as three other cages with filled pentagons (Fig. 2). We find that the core–shell and D_{3d} structures are lower in energy than the B_{80} buckyball structure at all DFT levels of theory (Table S1). Some DFT methods also predict the C_{3v} and T_h cages to be more stable than the buckyball structure. These results are generally consistent with the previous DFT studies.[25–31]

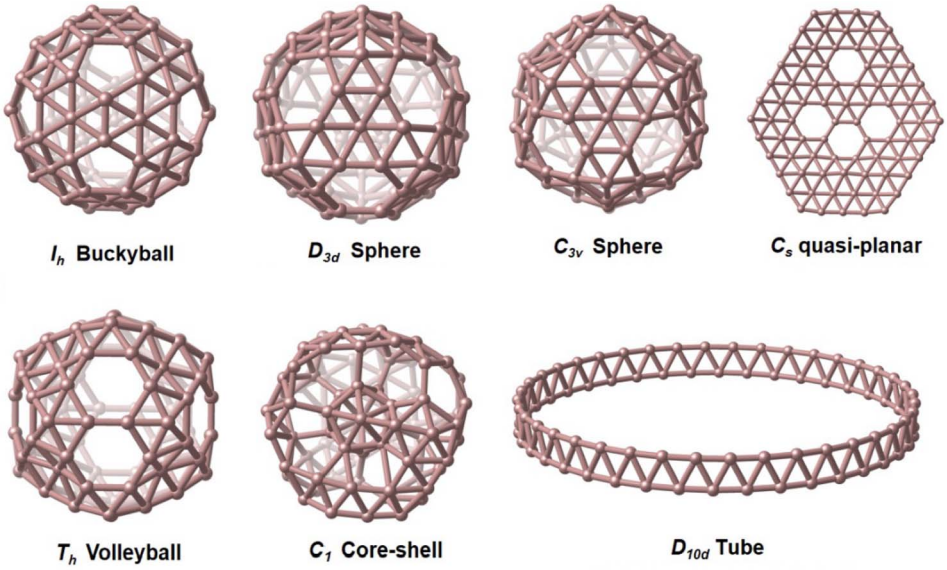

Fig. 2 Optimized structures for selected low-lying isomers of B_{80} (see Table S1).

3 Discussion

3.1 Simulated photoelectron spectra

To decipher the true global minimum, we simulated the photoelectron spectra of the selected isomers using the generalized Koopmans' theorem (see the SI). The simulated spectrum of the buckyball structure is compared with the experimental data in Fig. 1b, while those for the remaining six isomers are given in Fig. S4. The computed VDEs for the seven structures are given in Tables S2–S8. Remarkably, only the simulated spectral pattern of the D_{5d} B_{80}^- buckyball agrees with the experimental spectrum (Fig. 1). The three distinct spectral bands (X, A, and B) resolved experimentally are well reproduced in the simulated spectrum based on the buckyball structure. None of the simulated spectra for the other structures (Fig. S4) agrees with the experimental spectrum. Although it is difficult to completely rule out the presence of other isomers experimentally as minor species, their contributions to the observed spectrum would be expected to be negligible, if at all. Any substantial population of co-existing isomers would result in congested spectra and smear out the spectral features, as recently observed for B_{56}^-.[21]

We have analyzed the detailed electronic structure of the B_{80}^- buckyball (*vide infra*) and found that there is a one-to-one correspondence between the observed photoelectron spectral features and the valence molecular orbitals, as shown in Fig. S5 and also in Table S2. The high orbital degeneracies in the I_h B_{80} are lifted in the D_{5d} B_{80}^- anion due to the Jahn–Teller effect, but the energy level splitting is small and the bunching of the energy levels in the D_{5d} anion is still evident in Fig. S5 and Table S2. Thus, the well-resolved spectral features (X, A, and B) provide defining experimental electronic fingerprints for the high symmetry buckyball structure. Clusters from the laser vaporization source are formed under very hot conditions and then cooled down inside the nozzle before further cooling during the supersonic expansion. Kinetic trapping for a high energy isomer is unlikely in the laser vaporization cluster source. The stability of the buckyball structure is likely underestimated at the DFT level. In conclusion, the excellent agreement between experiment and theory confirms unequivocally that the buckyball structure is the global minimum for B_{80}^-.

3.2 The I_h *vs.* T_h symmetry for the B_{80} buckyball

Previous DFT calculations showed that the I_h B_{80} was not a minimum with imaginary frequencies and distorted to T_h symmetry,[35–37] in which 8 capping B atoms move away from the cage center while the other 12 capping B atoms move toward the cage center (Fig. S6). However, a previous MP2 calculation[38] and a dispersion-corrected DFT calculation[39] found that the I_h B_{80} is a true minimum and is more stable than the T_h B_{80}, suggesting that DFT methods cannot effectively describe the delicate electron correlation effects in B_{80}. We find similar issues with DFT methods in a previous study of the B_9^- cluster.[40] Our current DFT calculations are consistent with the previous DFT results for the B_{80} buckyball. At the B3LYP level, we find that the 8 capping atoms move above the plane of each hexagon by 0.26 Å, whereas the remaining 12 capping B atoms move toward the center of the cage by 0.22 Å (Fig. S6). However, at the MP2 level of theory, we find that the T_h B_{80} is no longer a minimum and it is optimized to the I_h structure, consistent with the previous MP2 result.[38] In addition, we also optimized an isomer with all capping B atoms above the center of the hexagons (outer-I_h) and another isomer with all the capping B atoms below the center of the hexagons (inner-I_h) (Fig. S6) and found that the capping atoms in both isomers move to the plane of the hexagons after optimization at the MP2 level of theory, indicating that the I_h structure with 20 B atoms sitting in the center of each hexagon is indeed the most stable configuration.

We observe that the B–B bond lengths in the DFT and MP2 calculations are significantly different (Table S9). At the B3LYP level, the B–B bond length between two adjacent hexagons is 1.665 Å and the B–B bond length around the pentagons is 1.738

Å. On the other hand, at the MP2 level the B–B bond length of 1.716 Å between two adjacent hexagons and the B–B bond length of 1.707 Å for the edges of the pentagons are similar. Thus, the hexagons are slightly too small in the B3LYP calculation to fit a B atom, similar to the out-of-plane distortion by the center atom in the C_{6v} B©B_6^- cluster.[41] We also optimized the structure of C_{60} at the B3LYP and MP2 levels (Table S10) and found that both levels of theory gave similar C–C bond lengths, which agree well with the experimental C–C bond lengths.[42] These results suggest that electron correlation effects are more complicated in the B_{80} buckyball than those in C_{60} and that DFT calculations likely underestimated the stability of the B_{80} buckyball.

3.3 The electronic structure of the B_{80} and B_{80}^- buckyball

The B_{80} buckyball is valence-isoelectronic to C_{60} and they have been shown to have the same occupied valence molecular orbitals (Fig. S7).[43–45] Similar to C_{60}, the LUMO of B_{80} is triply degenerate ($8t_{1u}$) and its HOMO is five-fold degenerate ($6h_u$). The HOMO–LUMO gap of C_{60} (1.62 eV)[32,46] is larger than the 0.8 eV value measured for B_{80} (Fig. 1a). In the anion, the extra electron occupies the $8t_{1u}$ LUMO. The ensuing Jahn-Teller distortion reduces the I_h symmetry of the neutral buckyball to D_{5d} for both B_{80}^- and C_{60}^- and splits all the degenerate molecular orbitals (Fig. S8). The triply degenerate LUMO ($8t_{1u}$) splits into the $9a_{2u}$ and $13e_{1u}$ orbitals in the anion, where the extra electron resides in the lower energy $9a_{2u}$ orbital. By virtue of the generalized Koopmans' theorem, the molecular orbital energy levels of B_{80}^- already display qualitative resemblance to the photoelectron spectrum (Fig. S5), underlying how the high symmetry and high electronic degeneracy lead to the simple photoelectron spectral pattern or how the simple spectral pattern provides the electronic fingerprint for the high symmetry structure.

Electron detachment from the $9a_{2u}$ orbital gives rise to band X in the photoelectron spectrum (Fig. 1 and S5). The five-fold degenerate HOMO of neutral B_{80} splits into the closely-spaced $12e_{1u}$, $4a_{1u}$, and $12e_{2u}$ orbitals in the anion. Electron detachment from these orbitals gives rise to band A. The HOMO-1 (11 h_g) of B_{80} splits into $12e_{2g}$, $10a_{1g}$, and $12e_{1g}$ in B_{80}^-, corresponding to band B in the photoelectron spectrum. The computed VDEs from these detachment channels using the generalized Koopmans' theorem are given in Table S2 and compared with the experimental data. Both bands A and B correspond to multiple detachment channels, consistent with their broad spectral widths. The simulated spectra are obtained by fitting each VDE with a unit-area Gaussian function with a width of 0.15 eV. A higher density of states can be seen at higher binding energies, consistent with the broad photoelectron features observed on the higher binding energy side (Fig. S5). The computed VDEs used to produce the simulated spectra for the other six low-lying isomers in Fig. S4 are given in Tables S3–S8. All these structures give rise to more complicated density of states.

3.4 Chemical bonding in the B_{80} buckyball

The chemical bonding in the soccer-ball-shaped C_{60} is straightforward. Each carbon atom with sp^2 hybridization forms three C–C σ bonds with its three neighbors on the surface

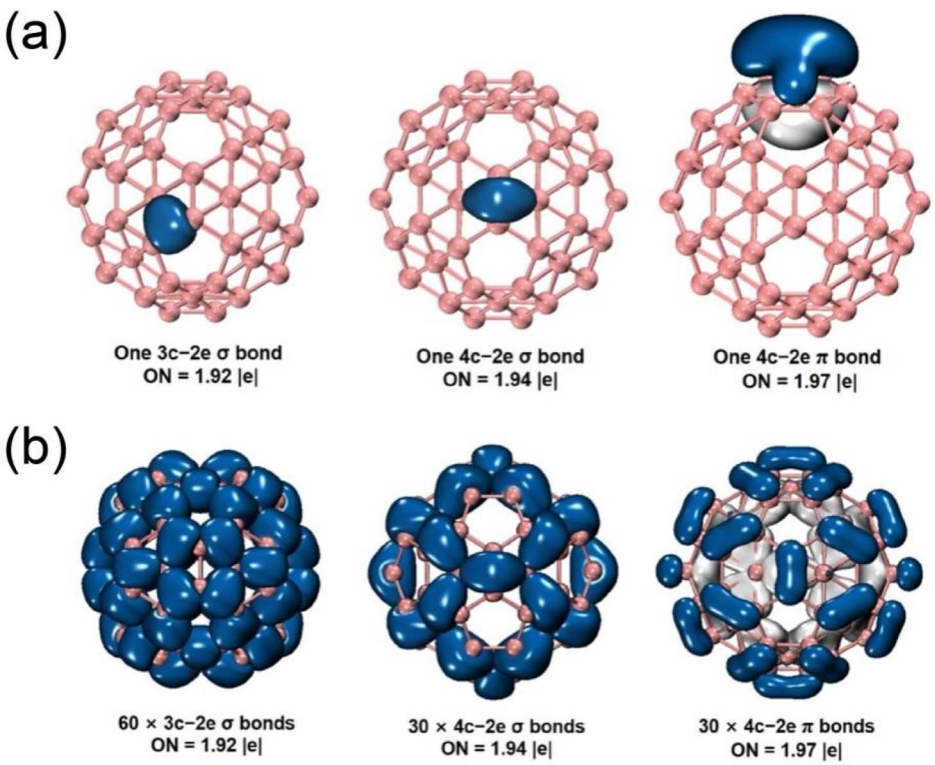

Fig. 3 Chemical bonding analyses for the B_{80} buckyball using AdNDP at the B3LYP/6-31G(d) level. (a) The three types of multi-center-two electron (*n*c-2e) bonds for the B_{80} buckyball. (b) The full sets of multi-center bonds for the B_{80} buckyball. The isovalue of 0.1 a.u. is used for all bonds, except for the 4c-2e π bond in (a), for which an isovalue of 0.02 a.u. is used to show more clearly the 4-center nature of this bond.

of the cage. The radial p_z orbital of each C atom then forms a π bond with a C atom on a neighboring pentagon, giving rise to the 30 double bonds shared between two adjacent hexagons. Thus, the 240 valence electrons in C_{60} form 90 C–C σ bonds and 30 C–C π bonds, which can be seen more clearly from the AdNDP analyses (Fig. S9).[47] Boron has the same number of valence orbitals, but is one-electron deficient relative to carbon. If an I_h B_{60} with 180 valence electrons were to form 90 B–B σ bonds, this structure would not be stable without the π bonds. Thus, filling each of the 20 hexagons with a B atom provides the 60 needed valence electrons, making B_{80} valence-isoelectronic to C_{60}. In the ionic bonding limit, the capping B atoms could be viewed as donating all its three valence electrons to the B_{60} framework to give rise to a B_{60}^{60-} buckyball interacting with 20 capping trivalent B atoms. Bonding analyses using B_{60}^{60-} and 20 hypothetical X^{3+} dummy ions indeed yield a bonding pattern identical to that of C_{60} (Fig. S10). While we find some degree of charge transfer from the capping B atom to the B_{60} framework in B_{80} (Table S11), it is not reasonable to expect complete charge transfer. The capping B atoms are expected to participate in multi-center covalent bonding with the B_{60} framework for both σ and π bonding in the B_{80} buckyball.

We use the AdNDP approach[47] to decipher the bonding in the B_{80} buckyball (Fig. 3). We find three types of multi-center two-electron (*n*c-2e) bonds: (1) 3c-2e σ bond, (2) 4c-2e π bond, and (3) 4c-2e σ bond. Fig. 3a shows an example of each type of the bonds, and Fig. 3b displays the full sets of the 60 3c-2e σ bonds, 30 4c-2e π bonds, and 30 4c-2e σ bonds. The 3c-2e σ bonds involve each of the edges of the pentagon and the capping atom in the adjacent hexagon. Thus, the 60 3c-2e σ bonds are exactly equivalent to the 60 single C–C bonds around the pentagons in C_{60} (Fig. S9b). The 4c-2e σ and π bonds involve the same four atoms including the B–B atoms shared between two hexagons and their two capping B atoms, corresponding exactly to the C=C double bonds in C_{60} (Fig. S9b). Thus, the structure and bonding of the B_{80} buckyball completely mimic that of the C_{60} buckyball, underlying its exceptional stability. Since the 4-center bonds contain two triangles, there is one electron pair on average for each of the 120 triangles on the surface of the B_{80} buckyball, consistent with the fact that all the B–B bond lengths are similar (Table S9).

4 Conclusion and perspective

The name buckminsterfullerene for C_{60} came from its structural similarity to the geodesic dome invented by Buckminster Fuller.[1] The surface of the geodesic dome consists of triangles by filling all the hexagons and pentagons. The I_h structure of B_{80} with filled hexagons is, in fact, closer to the real geodesic dome than C_{60}. The diameter of B_{80} is 0.85 nm, slightly larger than the 0.71 nm diameter of C_{60}, providing more flexibility to form endohedral compounds.[48,49] A molecular solid of B_{80} (boron fullerite) will be a new form of boron, like the fullerite.[50] The smaller HOMO–LUMO gap of the B_{80} buckyball suggests that the boron fullerite will be a semiconductor with an energy gap around 0.8 eV. Doping boron fullerite will turn it into a metal or even a superconductor, such as observed in the doped fullerite.[51] The high electron affinity of B_{80} suggests that it will be a better electron acceptor than C_{60}. Thus, boron fullerite may be a superior material for H_2 storage or lithium-ion batteries.[52] The B_{80} buckyball has also been shown to be able to react with small molecules on its surface,[53,54] suggesting that the boron buckyball should have much richer chemical and physical properties than its carbon counterpart.

Author contributions

H. W. C. led the experiment and analyzed the data. D. K. and H. W. G. helped with the experiment. Y. Y. Z. and C. Q. X. did the calculations; J. L. and L. S. W. guided the project and wrote the paper.

Conflicts of interest

The authors declare no conflict of interest.

Data availability

The data that support the findings of this study are available from the corresponding authors upon request.

Supplementary information (SI): additional experimental and computational data, including the 266 nm photoelectron spectrum, low-lying isomers of B_{80}^- and B_{80}, simulated spectra for selected isomers, comparison of the molecular orbital energy levels with the photoelectron spectrum, chemical bonding analysis for a model B_{60}^{60-} buckyball and C_{60}, and the Cartesian coordinates of the selected B_{80} isomers (PDF). See DOI: https://doi.org/10.1039/d6sc02674e.

Acknowledgements

L.S.W. would like to thank Prof. David Manolopoulos, Prof. David Tew, and Prof. David Wales for valuable discussions. The experimental work was supported by the U.S. National Science Foundation (CHE-2403841 to L.S.W.). The theoretical work was supported by the National Natural Science Foundation of China (Grant No. 22033005, 22503106, 92361302), NSFC Center for Single-Atom Catalysis (22388102), the National Key R&D Program of China (No. 2022YFA1503900), Natural Science Foundation of Jiangxi Province (Grant No. 20252BAC200032), and partially sponsored by the Guangdong Provincial Key Laboratory of Catalysis (No. 2020B121201002). The calculations were supported by Center for Computational Science and Engineering at Southern University of Science and Technology, CHEM high-performance supercomputer cluster (CHEM-HPC) at the Department of Chemistry, Southern University of Science and Technology (SUSTech) and supercomputers at the National Laboratory of Information Science and Technology of Tsinghua University.

References

1 H. W. Kroto, J. R. Heath, S. C. O'Brien, R. F. Curl and R. E. Smalley, *Nature*, 1985, **318**, 162–163.
2 S. Iijima, *Nature*, 1991, **354**, 56–58.
3 K. S. Novoselov, A. K. Geim, S. V. Morozov, D. Jiang, Y. Zhang, S. V. Dubonos, I. V. Grigorieva and A. A. Firsov, *Science*, 2004, **306**, 666–669.

4 H. J. Zhai, B. Kiran, J. Li and L. S. Wang, *Nat. Mater.*, 2003, **2**, 827–833.
5 A. N. Alexandrova, A. I. Boldyrev, H. J. Zhai and L. S. Wang, *Coord. Chem. Rev.*, 2006, **250**, 2811–2866.
6 A. P. Sergeeva, I. A. Popov, Z. A. Piazza, W. L. Li, C. Romanescu, L. S. Wang and A. I. Boldyrev, *Acc. Chem. Res.*, 2014, **47**, 1349–1358.
7 L. S. Wang, *Int. Rev. Phys. Chem.*, 2016, **35**, 69–142.
8 T. Jian, X. N. Chen, S. D. Li, A. I. Boldyrev, J. Li and L. S. Wang, *Chem. Soc. Rev.*, 2019, **48**, 3550–3591.
9 H. Bai, T. T. Chen, Q. Chen, X. Y. Zhao, Y. X. Zhang, W. J. Chen, W. L. Li, L. F. Cheung, B. Bai, J. Cavanagh, W. Huang, S. D. Li, J. Li and L. S. Wang, *Nanoscale*, 2019, **11**, 23286–23295.
10 B. Albert and H. Hillebrecht, *Angew. Chem., Int. Ed.*, 2009, **48**, 8640–8668.
11 A. R. Oganov, J. Chen, C. Gatti, Y. Z. Ma, Y. Ma, C. W. Glass, Z. Liu, T. Yu, O. O. Kurakevych and V. L. Solozhenko, *Nature*, 2009, **457**, 863–867.
12 Q. An, K. M. Reddy, K. Y. Xie, K. J. Hemker and W. A. Goddard, *Phys. Rev. Lett.*, 2016, **117**, 085501.
13 E. Oger, N. R. M. Crawford, R. Kelting, P. Weis, M. M. Kappes and R. Ahlrichs, *Angew. Chem., Int. Ed.*, 2007, **46**, 8503–8506.
14 B. Kiran, S. Bulusu, H. J. Zhai, S. Yoo, X. C. Zeng and L. S. Wang, *Proc. Natl. Acad. Sci. U. S. A.*, 2005, **102**, 961–964.
15 Z. A. Piazza, H. S. Hu, W. L. Li, Y. F. Zhao, J. Li and L. S. Wang, *Nat. Commun.*, 2014, **5**, 3113.
16 A. J. Mannix, X. F. Zhou, B. Kiraly, J. D. Wood, D. Alducin, B. D. Myers, X. Liu, B. L. Fisher, U. Santiago, J. R. Guest, M. J. Yacaman, A. Ponce, A. R. Oganov, M. C. Hersam and N. P. Guisinger, *Science*, 2015, **350**, 1513–1516.
17 B. Feng, J. Zhang, Q. Zhong, W. Li, S. Li, H. Li, P. Cheng, S. Meng, L. Chen and K. Wu, *Nat. Chem.*, 2016, **8**, 563–568.
18 H. J. Zhai, Y. F. Zhao, W. L. Li, Q. Chen, H. Bai, H. S. Hu, Z. A. Piazza, W. J. Tian, H. G. Lu, Y. B. Wu, Y. W. Mu, G. F. Wei, Z. P. Liu, J. Li, S. D. Li and L. S. Wang, *Nat. Chem.*, 2014, **6**, 727–731.
19 W. J. Chen, Y. Y. Ma, T. T. Chen, M. Z. Ao, D. F. Yuan, Q. Chen, X. X. Tian, Y. W. Mu, S. D. Li and L. S. Wang, *Nanoscale*, 2021, **13**, 3868–3876.
20 L. Sai, X. Wu, N. Gao, J. Zhao and R. B. King, *Nanoscale*, 2017, **9**, 13905–13909.
21 Q. Chen, H. W. Choi, G. F. Wei, D. Kahraman, R. N. Yuan, Q. W. Zhang, Q. Q. Yan, X. N. Zhao, C. Y. Gao, Y. Y. Ma, R. Wei, Y. Gui, Z. P. Liu, S. D. Li and L. S. Wang, *Proc. Natl. Acad. Sci. U. S. A.*, 2025, **122**, e2510702122.
22 X. Wu, R. Liao, X. Liang, L. Sai, Y. Liu, G. Yang and J. Zhao, *Nanoscale*, 2023, **15**, 10430–10436.
23 N. Gonzalez Szwacki, A. Sadrzadeh and B. I. Yakobson, *Phys. Rev. Lett.*, 2007, **98**, 166804.
24 D. L. V. K. Prasad and E. D. Jemmis, *Phys. Rev. Lett.*, 2008, **100**, 165504.
25 H. Li, N. Shao, B. Shang, L. F. Yuan, J. Yang and X. C. Zeng, *Chem. Commun.*, 2010, **46**, 3878–3880.
26 J. Zhao, L. Wang, F. Li and Z. Chen, *J. Phys. Chem. A*, 2010, **114**, 9969–9972.
27 S. De, A. Willand, M. Amsler, P. Pochet, L. Genovese and S. Goedecker, *Phys. Rev. Lett.*, 2011, **106**, 225502.
28 F. Li, P. Jin, D.-e. Jiang, L. Wang, S. B. Zhang, J. Zhao and Z. Chen, *J. Chem. Phys.*, 2012, **136**, 074302.
29 X. Q. Wang, *Phys. Rev. B*, 2010, **82**, 153409.
30 P. Pochet, L. Genovese, S. De, S. Goedecker, D. Caliste, S. A. Ghasemi, K. Bao and T. Deutsch, *Phys. Rev. B*, 2011, **83**, 081403.
31 J. T. Muya, E. Lijnen, M. T. Nguyen and A. Ceulemans, *Chem. Phys. Chem.*, 2013, **14**, 346–363.
32 S. H. Yang, C. L. Pettiette, J. Conceicao, O. Cheshnovsky and R. E. Smalley, *Chem. Phys. Lett.*, 1987, **139**, 233–238.
33 X. Chen, Y. F. Zhao, Y. Y. Zhang and J. Li, *J. Comput. Chem.*, 2019, **40**, 1105–1112.
34 W. L. Li, X. Chen, T. Jian, T. T. Chen, J. Li and L. S. Wang, *Nat. Rev. Chem.*, 2017, **1**, 0071.
35 G. Gopakumar, M. T. Nguyen and A. Ceulemans, *Chem. Phys. Lett.*, 2008, **450**, 175–177.
36 N. Gonzalez Szwacki, A. Sadrzadeh and B. I. Yakobson, *Phys. Rev. Lett.*, 2008, **100**, 159901.
37 T. Baruah, M. P. Pederson and R. R. Zope, *Phys. Rev. B*, 2008, **78**, 045408.
38 N. Gonzalez Szwacki and C. J. Tymczak, *Chem. Phys. Lett.*, 2010, **494**, 80–83.
39 R. N. Gunasinghe, C. B. Kah, K. D. Quarles and X. D. Wang, *Appl. Phys. Lett.*, 2011, **98**, 261906.
40 L. L. Pan, J. Li and L. S. Wang, *J. Chem. Phys.*, 2008, **129**, 024302.
41 A. N. Alexandrova, A. I. Boldyrev, H. J. Zhai and L. S. Wang, *J. Phys. Chem. A*, 2004, **108**, 3509–3517.
42 E. F. Sheka, B. S. Razbirin and D. K. Nelson, *J. Phys. Chem. A*, 2011, **115**, 3480–3490.
43 A. Ceulemans, J. T. Muya, G. Gopakumar and M. T. Nguyen, *Chem. Phys. Lett.*, 2008, **461**, 226–228.
44 A. Sadrzadeh, O. V. Pupysheva, A. K. Singh and B. I. Yakobson, *J. Phys. Chem. A*, 2008, **112**, 13679–13683.
45 Q. B. Yan, X. L. Sheng, Q. R. Zheng, L. Z. Zhang and G. Su, *Phys. Rev. B*, 2008, **78**, 201401.
46 X. B. Wang, H. K. Woo and L. S. Wang, *J. Chem. Phys.*, 2005, **123**, 051106.
47 D. Y. Zubarev and A. I. Boldyrev, *Phys. Chem. Chem. Phys.*, 2008, **10**, 5207–5217.
48 P. Jin, C. Hao, Z. Gao, S. B. Zhang and Z. Chen, *J. Phys. Chem. A*, 2009, **113**, 11613–11618.
49 J. T. Muya, E. Lijnen, M. T. Nguyen and A. Ceulemans, *J. Phys. Chem. A*, 2011, **115**, 2268–2280.
50 W. Kratschmer, L. D. Lamb, K. Fostiropoulos and D. R. Huffman, *Nature*, 1990, **347**, 354–358.
51 A. F. Hebard, M. J. Rosseinsky, R. C. Haddon, D. W. Murphy, S. H. Glarum, T. T. M. Palstra, A. P. Ramirez and A. R. Kortan, *Nature*, 1991, **350**, 600–601.
52 G. Wu, J. Wang, X. Zhang and L. Zhu, *J. Phys. Chem. C*, 2009, **113**, 7052–7057.
53 J. T. Muya, F. D. Proft, P. Geerlings, M. T. Nguyen and A. Ceulemans, *J. Phys. Chem. A*, 2011, **115**, 9069–9080.
54 Q. Sun, M. Wang, Z. Li, A. Du and D. J. Searles, *J. Phys. Chem. C*, 2014, **118**, 2170–2177.